IEEE Access
Multidisciplinary | Rapid Review | Open Access Journal

Received July 30, 2020, accepted August 12, 2020, date of publication August 25, 2020, date of current version September 9, 2020.

Digital Object Identifier 10.1109/ACCESS.2020.3019450

Assist-as-Needed Robotic Rehabilitation Strategy Based on z-Spline Estimated Functional Ability

SHAWGI Y. A. MOUNIS[1], NORSINNIRA ZAINUL AZLAN[1], (Member, IEEE), AND FATAI SADO[2], (Member, IEEE)

[1]Department of Mechatronics Engineering, International Islamic University Malaysia, Kuala Lumpur 50728, Malaysia
[2]Department of Mechanical Engineering, University of Malaya, Kuala Lumpur 50603, Malaysia

Corresponding author: Norsinnira Zainul Azlan (sinnira@iium.edu.my)

This work was supported by the Asian Office of Aerospace Research and Development (AOARD) for the Hardware and Control Algorithm Development under Grant FA2386-18-14105 RRD 18IOA105.

ABSTRACT Assist-as-needed (AAN) robotic-rehabilitation therapy is an active area of research which aims to promote neuroplasticity and motor coordination through active participation in functional task. A key component of this strategy is to provide robotic assistance to patients only when needed. To achieve this, accurate estimation of patients' movement/functional ability (FA) is required to evaluate patients' need for robotic assistance and to provide the required amount of assistance, which is still a significant challenge to AAN robotic-rehabilitation therapy. This study proposes an AAN technique based on a new Functional Activity Spline Function (FASF) to estimate patients' FA and to adapt robotic assistance. The FASF is formulated using z-spline curve to estimate patients' movement ability based on the quality-of-movement and the time score of the patient in each functional task. A Linear Quadratic Gaussian Integral (LQGi) torque controller is applied with a FASF-to-torque mapping algorithm to physically provide low-level torque assistance on the elbow/shoulder joints. Fifteen patients were involved in the experimental study which consists of two tasks: (Task1) a pick-and-place task and (Task2) a table-to-mouth reaching task. The results showed that the proposed ANN control strategy has successfully estimated the patients' FA consistently with high repeatability, and able to provide the robotic assistance according to the patients' needs in the task. For different levels of impairment, the average percent-torque assistance across trials relative to the highest possible assistive torque are within the range of 5.43%-24.85% (for the mildly impaired) and 75.14%-97.14% (for the severely impaired) patents in both reaching task consistent with their FA estimation.

INDEX TERMS Assist-as-needed (AAN), rehabilitation therapy, functional capability, stroke, impairment, z-spline function, a linear quadratic Gaussian (LQG), torque assistance and hybrid finite state automata.

I. INTRODUCTION

Stroke is a leading cause of disability world-wide [1], [2]. It significantly reduce patients' functional ability and performance of activities of daily living (ADL) [3]. Statistics show that about 80% of people with acute stroke manifest upper limb motor impairment accompanied with reduced arm function [4]. Even 4 years early after stroke, about 50% would still have functional impairments [4]. Regaining patients' functional ability after stroke is the primary focus of physical and occupational therapy [5]. Early therapy after stroke usually include passive exercise training to prevent muscle atrophy and to relieve joint contractures [6]. However, as the training progresses, active participation is encouraged to provoke neuroplasticity of affected regions of the nervous system and to improve patient functional ability [7], [8].

Clinical studies have suggested that, for patients who have regained parts of their motor functions [9], a rehabilitation treatment integrated with voluntary efforts of patients facilitates recovery of lost motor ability [10]. Thus, assisting every movement of the patients is not found to be beneficial compared to when they are actively involved in the exercise [11]. Active training requires cognitive processing which stimulates neuroplasticity and thus achieve greater gains in performance than movement training that did not encourage cognitive processing [12], [13].

Assist-as-needed robotic therapy is currently a driving trend in robot-aided rehabilitation therapy [14] that emphasizes patient active participation [15]. Under the assistive scheme, the patient performs the prescribed task

The associate editor coordinating the review of this manuscript and approving it for publication was Yu-Huei Cheng.

independently whereas the robot should provide assistance to aid the patient only when it is deemed necessary otherwise it withholds the assistance [16]. Some AAN scheme introduces a baseline minimal robotic assistance that is first provided to the patients to assist on the exercise and thereafter the robot decreases the assistance according to the patients' need or movement ability thus adapting assistance to the patient's functional capability [17].

Several studies have attempted to implement AAN strategies in robotic therapy however, a major challenge is how to effectively determine patients' movement ability or performance in order to adjust robotic assistance and also to determine the amount of assistance required [18], [19]. Considering the method of extracting information from the patient (patient specific movement information), two major classifications are possible: (kinematic or biomechanics) sensor based methods and model-based approaches [8], [20]. Krebs *et al.* [21] first implemented a performance-based progressive robotic therapy with MIT-Manus that uses kinematic and biomechanics information from sensors, namely speed, time, and EMG thresholds, to initiate robot assistance. The patient's performance was determine using the patient's active muscle power and motion accuracy [21], [22]. EMG activity in 14 muscles of the shoulder and elbow was used to calculate patients' muscle power and consequently the stiffness of the robot controller was adjusted based on the patient's performance in the last reaching movement [21]. Papaleo *et al.* [23] proposed a patient-tailored adaptive therapy for an upper limb rehabilitation robot that includes a module for evaluation of patients' performance based on biomechanical data. The patients' biomechanical data were recorded from sensory system (i.e. from encoders embedded in the robot, magneto-inertial sensor, and accelerometer placed on the patient arm). By this means, the module produces a discrete response for updating control parameters (i.e. stiffness and task duration), which allow modulation of robotic assistance and task complexity. Another sensor based approach was proposed by Vergaro *et al.* [24] using a force field generator, a performance evaluation module, and an adaptive controller. The force field generator uses an impedance control scheme which rely on kinematic sensor information from the robot (e.g. angles and angular velocities). Performance evaluation is achieved by stipulating some performance criteria to obtain a patient score at the end of each session. Consequently, the controller progressively decreases the gain of the force field, within a session, and propagates the minimum gain achieved in a session to the next session. Other sensor-based adaptive techniques include the adaptive impedance method proposed by Pérez-Ibarra *et al.* [25] which estimate patients' contribution from torque and kinematic information during the motion and adapt the robotic assistance based on patient's performance in a video game. Another is the reinforcement learning-based impedance controller that actively reshapes the stiffness of the force-field to the subject's performance, while providing assistance only when needed. The proposed controller is built upon action dependent heuristic dynamic programming using the actor-critic structure, which does not require prior knowledge of the system model but the kinematic error between reference trajectory and the actual trajectory of the system.

In contrast with these scheme, Wolbrecht *et al.* [26] proposed a model-based approach using a standard model-based, adaptive control technique to learn the subject's abilities and to assist in completing movements while remaining compliant. The assist-as-needed scheme is consequently achieved by adding a novel force reducing term to the adaptive control law, which decays the force output from the robot when errors in task execution by subjects are small [26]. Pehlivan *et al.* [8] also proposed a model-based approach under a minimal assist-as-needed mAAN strategy. The authors applied a Kalman-based sensor-less force estimation technique which determines a disturbance term corresponding to subjects' functional input in reaching task. The estimated functional input is then applied to update the derivative feedback gain which consequently modify the bounds of allowable error on the desired trajectory, allowing subject-tailored participation. Other model-based adaptive control techniques emphasize learning controller or model parameters to adapt the robotic assistance. An example is the strategy proposed by Bower *et al.* [27] that learns a state-dependent model of participant utilizing an unstructured inertial model that depends on the position and direction of the desired motion in the robot's platform. The approach learns a patient impairment model that accounts for movement specific disability in neuromuscular output and combined with assist-as-needed force decay to promote more engagement and participation from the patients. Other examples include the RL framework used in [28] which learns the sensitivity factor of the system model in order to reduce physical human robot interactions, and the AAN controller framework proposed by Obayashi *et al.* [29] that uses a RL algorithm to adjust the stiffness of an IC in order to help subjects learn a dart-throwing task. Another noteworthy AAN adaptive control (hierarchical compliance) strategy by Liu *et al.* [30], proposed for the soft ARBOT, and it suggests a method to estimate the subject's active ankle torque and movement performance by monitoring the subject's active participation online adapted to the individual's behavior and ability.

Some of the merits of model-based approach is that they could minimize cost of equipment and enhance compliance but their heavy reliance on the accuracy of the robot model constitute a potential limitation in terms of remodeling for different robotic systems, and inaccurate estimation of subjects' abilities due to model excitation errors. This would lead to inconsistencies in estimation for a wide subject population [27].

So far, finding an appropriate estimation strategy for patients functional/movement ability under an AAN scheme that is consistent and repeatable for a wider patient's population, and is consistent with clinical procedures is still an unresolved aspect of AAN research [5]. In this article,

we propose an assist-as-needed robotic rehabilitation technique based on a new functional activity spline function (FASF) which sufficiently and consistently estimate patients' movement activities in functional task to adapt robotic assistance. Our strategy is sensor-based, however, unlike previous sensor-based strategies proposed by Krebs *et al.* [21], Papaleo *et al.* [23], and Vergaro [24] the FASF algorithm proposed in this study applies a z-spline curve to estimate patient's movement ability based on patient's quality of movement and the time score in each functional task, much similar to the conventional clinical procedures of estimation of functional activity (e.g. the Action Research Arm Test (ARAT), WMFT, etc.). Thus, the main contribution of this work is to bridge the gap between the clinical procedure and robotic approach of estimation of patient functional/ movement ability, allowing consistencies or wider patients' population and allowing clinical procedure to be automated in robotic therapy. For this particular implementation, the baseline controller is a Linear Quadratic Gaussian (LQG) torque controller with integral action for robustness. Output of a FASF-to-torque mapping algorithm is coupled to the LQG controller to physically provide low-level torque assistance on the elbow and shoulder joint during reaching tasks.

The main contributions of this paper are:

1) A new novel patient's functional ability estimation function, known as the Functional Activity Spline Function (FASF) that is directly related to actual clinical assessment methods for estimating functional capability.

2) A new Assist-as-Needed control strategy that is based on the FASF algorithm, which is capable to regulate the amount of robotic assistance.

The rest of this paper is organized as follows: the hardware description and system modeling are specified firstly in section II, followed by the control architecture given as section III, experiment provided in section IV, results and discussions in section V and finally the conclusion is given in section VI.

II. HARDWARE DESCRIPTION AND SYSTEM MODELING

A. MECHANICAL SYSTEM

The prototype of the robotic device is shown in Fig.1. The device is five degrees of freedom (5-DOF) upper-limb rehabilitation system with 1-DoF at the shoulder, 1-DoF at the elbow, 1-DoF at the forearm, and 2-DoF at the wrist joints allowing the possibility of performing several upper-extremity reaching tasks. The device allows abduction/adduction (AA) movement of the shoulder joint, flexion/extension (FE) movement of the elbow, pronation/ supination (PS) movement of the forearm, and flexion/ extension (FE) and abduction/adduction (AA) movement of the wrist joints.

For actuation, two back-drivable brushless DC motors (Maxon RE50, 370955, 200W, 36 V) with a gear ratio of 1:113 are used for actuation of the shoulder and elbow joints. Brushless DC motors are specially chosen to offer

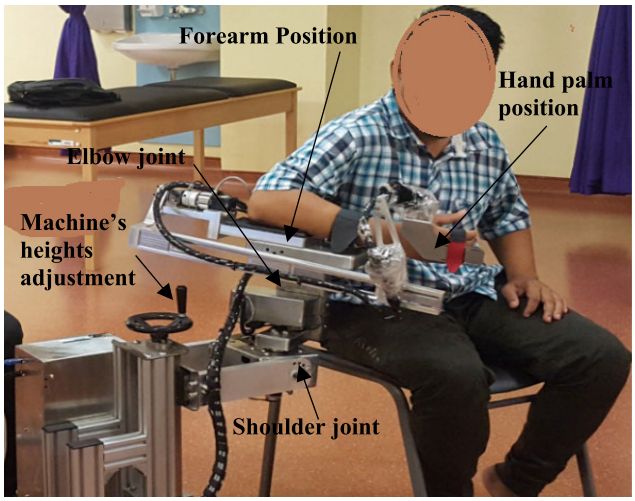

FIGURE 1. The upper limb rehabilitation exoskeleton.

low noise, low friction, low backlash, and compact size. The rest of the joints are passive to allow the possibility of performing several reaching tasks. Torque sensors with strain gauge mechanism are coupled on each joint to measure the total joint torque. To determine the joint position and range of motion, rotary type potentiometers are also attached at each joint.

B. FRICTION MODEL

Joint stiffness and frictional torques are estimated and applied in a feed-forward loop to the LQG torque controller to compensate the model uncertainties due to the joint friction (see Fig. 3.). The stiffness and frictional torque model is given by the method proposed in [31]:

$$\tau_f(q,\dot{q}) = \begin{cases} b_0 & q = 0,\ \dot{q} = 0 \\ b_1 sgn(\dot{q}) + b_2(\dot{q}) & \dot{q} = 0 \\ \tau_s(q) & q \neq 0,\ \dot{q} = 0 \end{cases} \quad (1)$$

where τ_f is torque friction, b_0 is the static friction torque; q is the 5×1 vector of joint angle position, $\dot{q}$ is the 5×1 vector of joint angular velocity, $b_1 sgn(\dot{q})$ is the coulomb or kinetic friction torque: a signed function of the joint angle velocity; and $b_2(\dot{q})$ is the damping friction torque: a function the upper limb rehabilitation exoskeleton of the joint velocity. $\tau_s(q)$ is the stiffness torque which is a function of joint angle position. Table 1 presents the estimation of the friction and stiffness torque parameters for the shoulder and elbow joints respectively.

C. SYSTEM IDENTIFICATION

In control application, system identification represents a quick approach to obtaining a dynamic model or transfer function of joints of a multi-body robotic system [32]. It is particularly useful in some occasion where representation of the system dynamically is not available. In this study, to obtain the transfer function of joints of the device, the sine-by-sine method is applied with a periodic band limited input

TABLE 1. Parameters and models of joint friction and stiffness torque.

Joint no. (q)	Static Friction Torque	Stiffness Torque	Damping Friction Torque
elbow	$\tau_{static} = 0.27\ N\ m$	$\tau_{stiffness} = 0.00018.\theta + 4.1\ Nm$	$\tau_{\text{dynamic}} = 0.00044.\dot{\theta} + 8.3\ Nm$
shoulder	$\tau_{static} = 0.21\ N\ m$	$\tau_{stiffness} = 0.00011.\theta + 2.7\ Nm$	$0.00031.\dot{\theta} + 6.13\ Nm$

excitation signal given by

$$i(t) = i_0 \sin\left(w_f t\right) \tag{2}$$

where i is the motor current, i_0 is the signal amplitude selected in the range [−0.5A 0.5A] of rated motor current, w_f is the fundamental frequency selected in the range [4π 8π] rad/s based on the overall model sampling time and t is the sampling time. Fig.2a and Fig. 2b. show the simulated and measured responses for the different sine-wave input applied to the shoulder joint and elbow joint respectively. The red bold line (Fig 2a) and the blue bold line (Fig. 2b) indicate the best fit model for both joints respectively. Other lines are given according to their percentage of fitting in Table 2 and Table 3.

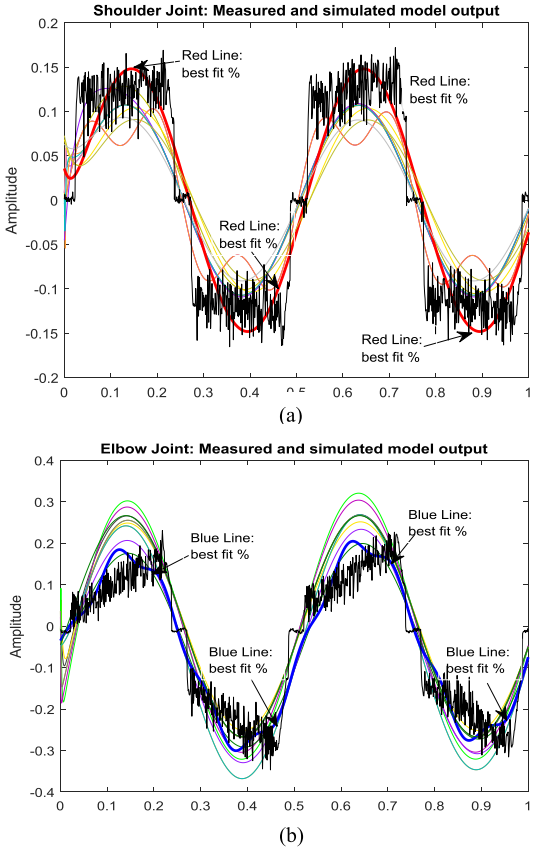

FIGURE 2. Simulated and measured responses for the different sine-wave input applied to the (a) shoulder joint and (b) elbow joint. Red line curve indicates best fit in (a) and blue line curve indicates best fit in (b).

TABLE 2. Estimated models for shoulder joint.

Line Color	Model	Fit (%)
Gray	$\frac{11.57s - 59.43}{s^2 + 24.5s + 0.0043}$	50.93
Red	$\frac{659.3 + 1240}{s^3 + 0.96s^2 + 1399s + 1140}$	69.30
light Blue	$\frac{49.89s + 423.9}{s^2 + 50.45s + 887}$	57.94
Orange	$\frac{-3.51s + 616}{s^2 + 5.14e^{-6}s + 1399}$	60.45
Purple	$\frac{150.5s + 8.87e^2}{24.89s^2 + 4.4e^{02}}$	58.03
Yellow	$\frac{152.5s - 2331}{s^3 + 52.83s^2 + 562.9s + 0.0005}$	52.64
light Purple	$\frac{1.2e^4s + 2.422e^5}{s^4 + 22.33s^3 + 1927s^2 + 2.1e^4s + 7.44}$	63.45
light Green	$\frac{-3693s + 5.6e^5}{s^4 + 44.82s^3 + 1848s^2 + 6.2e^4s + 6.4e}$	58.37
Orange	$\frac{274.2s^2 - 429.9s + 2.4e^5}{s^3 + 204.8s^2 + 1446s + 2.9e^5}$	57.62

TABLE 3. Estimated models for elbow joint.

Line Color	Model	Fit (%)
Blue	$\frac{5.07e^4s - 1.149e^5}{s^4 + 22.9s^3 + 4024s^2 + 9.1e^4s + 9.38e^4}$	68.87
Purple	$\frac{22.02s - 19.6}{s^2 + 34.7s + 34.47}$	58.41
light Green	$\frac{24.38}{s + 49.93}$	41.32
light Black	$\frac{216.1}{s^2 + 6.432s + 557.2}$	51.45
Yellow	$\frac{0.443s + 0.42}{s + 0.98}$	54.65
Orange	$\frac{24.17s - 35.49}{s^2 + 33.62s + 31.78}$	46.54
Black	$\frac{-340.6s^2 + 1.12e^5s - 2.5e^5}{s^4 + 26.28s^3 + 7672s^2 + 2s + 1.8e^5}$	50.29
Dark Green	$\frac{17.88s - 15.7}{s^2 + 31.99s + 29.68}$	65.63
light Purple	$\frac{325.6s + 126.1}{s^3 + 6.43s^2 + 51.3s + 354.5}$	42.26

III. AAN CONTROLLER ARCHITECTURE

The overall AAN control system architecture is depicted in Fig.3. The objective of the control is to adjust robotic assistance to patient's functional movement capability in reaching tasks (table-to-mouth and pick and place tasks). Such that assistance is provided only when the patient's functional ability (FA) is low and decreased until completely withdrawn when patient's FA improves. The AAN controller integrates three controller algorithms in a hierarchical structure: the FA algorithm for estimation of patients' functional ability, the hybrid finite state automaton to provide high-level coordination of the various reaching tasks, and the low-level LQG integral torque control algorithm to physically provide torque assistance. The following subsection provides more discussion.

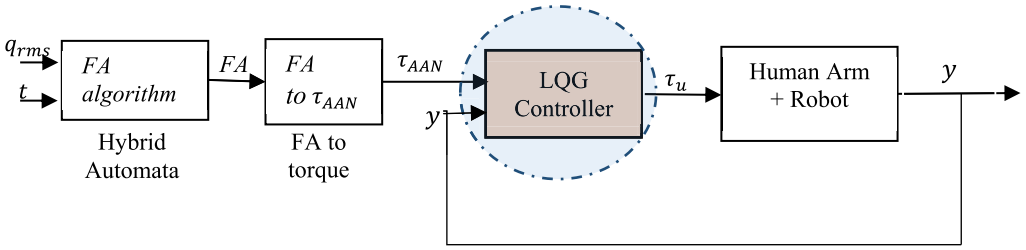

FIGURE 3. Control Architecture of the proposed AAN control strategy based on FA estimation algorithm.

A. FA ALGORITHM

The proposed FA algorithm is a new functional activity spline function (FASF) to accurately estimate patients' movement ability during functional activities. The motivation for the current approach is to find an appropriate robotic method of scoring patients FA that allows real time automation in robotic therapy, which is quite uncommon and challenging. Patients with severe case of neurological impairment perform very poorly on the time scale, whereas those with much better motor control ability have tendencies to complete reaching task much more quickly (typically less than 10secs). The variability in patients' functional ability based on their time score thus approximates a z-spline distribution curve with almost flat response at each limit of the curve. Fig.3 shows a typical curve of patients' functional activities based on time score adapted from the work of [33]–[36] and a z-spline interpolated curve.

In this study, we define the functional movement ability of the patients' based on the z-spline. Following clinical procedure, the indices for evaluation are the time score and quality of patients' movement. These indices serve as the input to the z-spline function to estimate patient's functional ability in real time making it suitable for application in robotic therapy. For assessment, we apply two clinical scales: Action research arm test (ARAT) for time score and wolf motor function test (WMFT) for quality of movement, which have proven consistency and inter-rater reliability. The ARAT scale rank patients' functional movement ability level in the range 0 – 3 based on time score and WMFT give the FA score based on quality of movement in reaching task, see Table 4. In our previous work [37], we have used the statistical normalization function for patient's functional ability. This approach had limitation because it assumes the distributions of patient's functional ability to be linear and also does not allow real time implementation in robotic therapy. The z-spline polynomial function adopted in the current study circumvent this limitation. With the polynomial splines function, the interval $[\boldsymbol{a}, \boldsymbol{b}]$ of each continuous function can be approximated arbitrarily.

Given the z-spline function shown in Fig. 4, we define the FASF, i.e. $\boldsymbol{FA}(\boldsymbol{q}, \boldsymbol{t})$ as

$$\boldsymbol{FA}(\boldsymbol{q},\boldsymbol{t}) = \frac{\boldsymbol{N}}{\boldsymbol{2}}(\emptyset_{\boldsymbol{t}} + \emptyset_{\boldsymbol{p}}) \tag{3}$$

$\emptyset_t$ and $\emptyset_p$ are the time score and quality of movement (QoM) respectively,

TABLE 4. ARAT-adapted functional ability scale (FAS).

FA	TIME SCORE t_p* (s)	QoM (q_{rms}) (m\m)	Remark
0	T_0	*~ 0.7 - 1*	0= Indicates no attempt to use the more affected upper limb hand
1	T_1	*~ 0.4 – 0.7*	1= performs the test partially, If a patient takes more than 60s to perform an task, the evaluator should interrupt after 60s and a score of 1 is given on that specific task.
2	T_2	*~ 0.1 – 0.4*	2 = completes the test, but takes an abnormally long time, varying from 8s to 60s.
3	T_3	*< 0.1*	3= performs the test normally in less than 5s.

* $T_0 \coloneqq t_p \geq 120$s; $T_1 \coloneqq 61\text{s} \leq t_p \leq 115.3$s; $T_2 \coloneqq 5\text{s} \leq t_p \leq 60$s; $T_3 \coloneqq t_p \leq 5$s

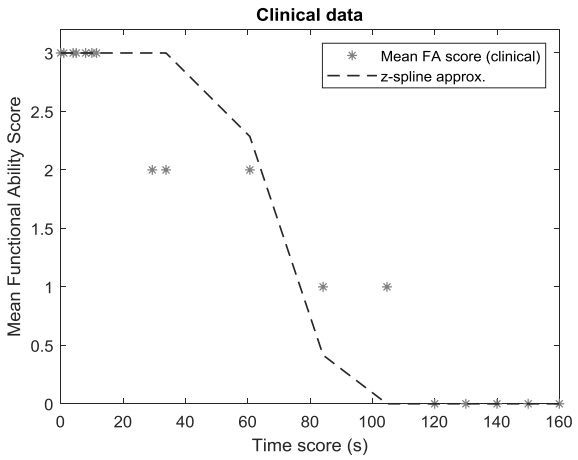

FIGURE 4. Time scores based on ARAT, The broken lines represent z-spline approximation.

where $\emptyset_t$ is given as:

$$\emptyset_t = \boldsymbol{N}.\boldsymbol{zmf}\,(\boldsymbol{t},(\boldsymbol{t_h}, \boldsymbol{t_{limit}})) \tag{4}$$

and:

$$\emptyset_p = \boldsymbol{N}.\boldsymbol{zmf}\,(\boldsymbol{q_{rms}}, (\boldsymbol{q_{hrms}}, \boldsymbol{q_{limitrms}})) \tag{5}$$

$\boldsymbol{t}$ is the time taken to complete a task, $\boldsymbol{t_h}$ is the corresponding time an healthy participant would take to complete the same

task, t_{limit} is the maximum time given to complete the task, q_{rms} is the quality of movement measured as root mean square, q_{hrms} is the quality of movement measured as a root mean square deviation from the trajectory profile of healthy participant, $q_{limit\,rms}$ is the maximum root mean square that can deviate from the reference trajectory, zmf is z-spline function, and N is the highest functional ability level (i.e. $N = 4$ for the ARAT). The z-spline function, $zmf(x,a,b)$ is defined as

$$zmf(x,a,b) = \begin{cases} 1, & x \le a \\ 1-2\left(\frac{x-a}{b-a}\right)^2, & a \le x \le \left(\frac{a+b}{2}\right) \\ 2\left(\frac{x-b}{b-a}\right)^2, & \left(\frac{a+b}{2}\right) \le x \le b \\ 0, & x \ge b \end{cases} \quad (6)$$

where $x = t$ or q_{rms} is the continuous variable. [a, b] represent any interval on the continuous function, which stands for the interval between the two regions of flat response behavior in this case (Fig. 4).

B. FA - TORQUE MAPPING ALGORITHM

As seen in Table 4, the FA score is given from 0 to 3 which corresponds to the levels of functional ability. To generate smooth reference torque based on the functional ability level, an FA-to-torque mapping algorithm is proposed in this section. The algorithm is defined to assign minimal torque assistance sufficient to complete a task and to map to a lower torque assistance should the patient show more functional capability. For patients or healthy subjects with significant functional capabilities, the algorithm ensures that a reference resistance torque is derived to resist the movement of the patient. Thus, the algorithm ensures that minimum assistance is given to a patient with significant functional disabilities and decreased to the point of resisting patients with more functional capabilities.

Given the FA score from the preceding section, the reference torque assistance is proposed as

$$\tau_{AAN} = \tau_0 \left(1 - \mathcal{F}(\mathrm{q_{rms}}, \mathrm{t})\frac{k}{N}\right) + \tau_f\,(q, \dot{q}) \quad (7)$$

where τ_{AAN} is the reference input to the torque controller, τ_0 is the starting torque assistance given to the severe disability level, $\tau_f\,(q, \dot{q})$ is the frictional torque, and the constant k is given as:

$$k = \begin{cases} 1, & \textit{if resistance is not included} \\ 2, & \textit{resistance provided} \end{cases} \quad (8)$$

C. LQG TORQUE CONTROLLER WITH INTEGRAL ACTION

1) CONTROLLER DESIGN

Typical system dynamics for LQG control are given by the stochastic state space equation of the open-loop plant. The state space equations are described by the complete system and output equations and can be written as follows:

$$\dot{\tau} = A\tau + B\tau_u + w \quad (9)$$

$$y = C\tau + v \quad (10)$$

where $\tau = [I, \dot{I}]^T$ is a 2×1 vector of states of the motor-joint-link system. I and $\dot{I}$ are the motor current and the derivative of the current respectively. The $A, \geq$ B, and C are the states matrices. τ_u is the control input to the motor and y is the output current of the motor. w and v are disturbance input and measurement noises, respectively, which are assumed white Gaussian noises with zero mean and covariance matrices W and V i. e

$$Q = E\,(wwT)\,, \quad R = E(vvT) \quad (11)$$

It is assumed w, v are not correlated with each other, hence $E(wvT) = N$.

Given the above plant, the LQG torque controller with output-states feedback and integral action is therefore designed as

$$\dot{\hat{\tau}} = A\tau + B\tau_u + L(y - C\hat{\tau}) \quad (12)$$

where L is the Kalman gain calculated to stabilize the output observation error $(y - C\hat{\tau})$, and control input is

$$\tau_u = -k\left[\hat{\tau}, \tau_i\right]^T = -k_\tau\hat{\tau} - k_i\tau_i \quad (13)$$

where $K = [k_\tau, k_i]$ is the 1×2 optimal gain matrix, $\hat{\tau}$ is the Kalman estimate of the system states, τ_i is the integrator states given by

$$\dot{\tau}_i = \tau_{AAN} - y = \tau_{AAN} - C\tau \quad (14)$$

where τ_{AAN} is the reference input to the LQG torque controller defined in Eqn. (7), Kalman gain L is determined by solving an algebraic Riccati equation given by:

$$L = (PC^T + \bar{N})\bar{R}^{-1} \quad (15)$$

where P is the state covariance matrix given by:

$$P = E[(\tau - \hat{\tau})(\tau - \hat{\tau})^T] \quad (16)$$

$$\bar{R} = R + HN + N^T H^T + (HQH)^T \quad (17)$$

$$\bar{N} = G((QH)^T + N) \quad (18)$$

where Q is covariance matrix of the disturbances (Eqn. 11), R is the covariance matrix of the measuring noise (Eqn. 11), and H is the eigenvectors.

The optimal gain matrix K on the other hand is obtained at the point where the feedback law minimizes the quadratic cost function given by

$$J(u) = \int_0^\infty \left\{x^T Qx + 2x^T Nu + u^T Ru\right\} dt \quad (19)$$

where $\bar{z} = [\hat{\tau}, \tau_i]^T$

Fig. 3 shows the overall proposed control strategy in this research work with the LQG representing a baseline low level controller.

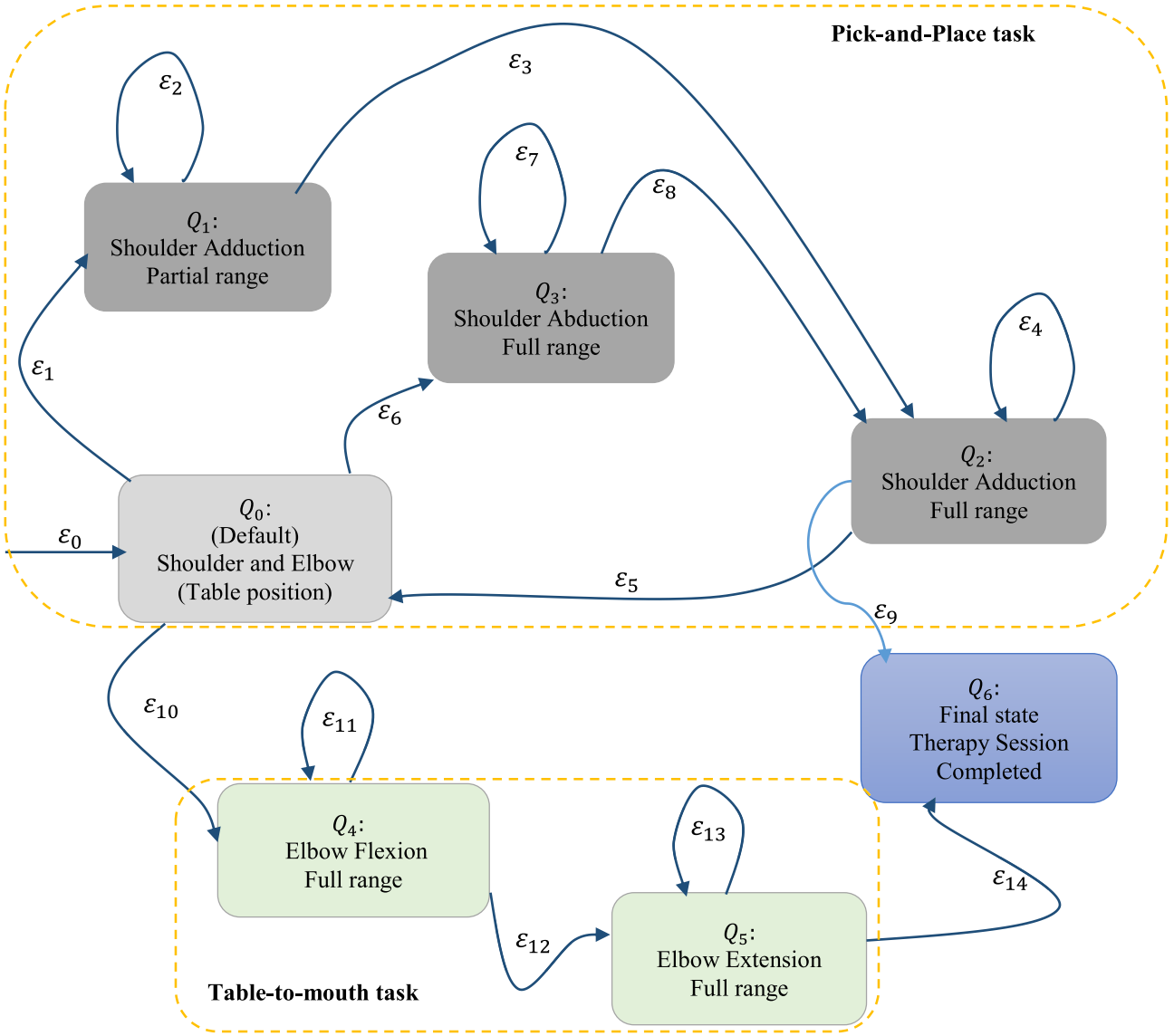

FIGURE 5. Finite state hybrid automaton transition.

D. HYBRID FINITE STATE AUTOMATA

To effectively automate and execute the FA estimation algorithm, a six-state hybrid automaton (see Fig. 5) is proposed and implemented here as a high-level supervisory controller. The hybrid finite state automata is used to ensure effective timing for each task and transition between tasks. Patients' functional activity is computed immediately after each task and is used to compute the assistive torque in the next task. This process requires effective timing and accuracy; thus, hybrid automata is implemented in this study. The automaton describes a mix discrete and continuous dynamic system formally defined as a tuple $\mathcal{H} = (Q, X, R, \varepsilon, x_0, Q_m)$ where

- Q is the set of discrete mode/state representing the different phases of each task as shown in Fig.5 /Table 5
- X defines the continuous state space. This represent
- the FA algorithm (i.e. Eqn. 3) in this context.
- R defines the set of control symbols generated by the FA algorithm. The output control symbols R varies according to the functional activity time score $\emptyset_t$ and the quality of motion $\emptyset_p$. Thus, $\emptyset_t$ measures how long a patient is able to complete a given task mode.
- ε represent the state transition function or jump or guard conditions given in Table 5
- x_0 is the initial condition, and
- Q_m represent the default state Q_0 or marked state Q_6.

Table 5 and 6 presents the states and transition/event logic, respectively, of the hybrid automaton shown in Fig. 5. The default state Q_0 marks the initial state of the hybrid automata where the patient's hand/arm is resting on the table. Transition from the default state to the other states Q_1 to Q_6 is made possible by the jump conditions (or events) ε. Two types of events/jumps are triggered in the automata: (1) the

TABLE 5. Transition logic states.

Transition (ε)	Transition logic	Transition (ε)	Transition logic
ε_0	Default transition	ε_8	$q - q_{Q_3} > \lambda,\ t > \beta = 60,\ F = \epsilon_8$ transition from one state to another
ε_1	$q - q_{Q_0} > \lambda,\ t > \beta$ $F = \epsilon_1$ transition from one state to another	ε_9	(trial $\geq$ ntrials) transition from one state to another
ε_2	Intra-state jump $t > \beta = 30$ transition to the same state	ε_{10}	$q - q_{Q_0} > \lambda,\ F = \epsilon_{10}$ transition from one state to another
ε_3	$q - q_{Q_1} > \lambda, t > \beta = 30,\ F = \epsilon_2$ transition from one state to another	ε_{11}	transition to the same state $t > \beta = 60$
ε_4	Intra-state jump $t > \beta = 60$ transition to the same state	ε_{12}	$q - q_{Q_4} > \lambda, t > \beta = 60,\ F = 12$ transition from one state to another
ε_5	$q - q_{Q_2} > \lambda, t > \beta = 60,\ F = \epsilon_5$ transition from one state to another	ε_{13}	transition to the same state $t > \beta = 60$
ε_6	$q - q_{Q_2} > \lambda,\ t > \beta$ $F = \epsilon_6$ transition from one state to another	ε_{14}	$q - q_{Q_5} > \lambda$, if (trial $\geq$ ntrials) transition from one state to another
ε_7	transition to the same state $t > \beta = 60$		

TABLE 6. Event logic.

Joint	Shoulder	
States	Task	Joint Movement
Q_0	Default position	Default position
Q_1	Pick a bottle From Table position–and-place it to another table position	Partial shoulder Adduction
Q_2	Pick From Table position–and-place to another table position	Full shoulder Abduction
Q_3	Pick From Table position–and-place to another table position	Full shoulder Adduction
Joint	Elbow	
States	Task	Joint Movement
Q_0	Default position	Default position
Q_4	Table-to-Mouth	Flexion
Q_5	Mouth-to-Table	Extension
Q_6	Table-to-Mouth	End, Therapy Completed

event that causes transition from one state to another (i.e. ε_1, ε_3, ε_5, ε_6, , ε_8, ε_9, ε_{10},, ε_{12}, ε_{13}, ε_{14}) and (2) the event that causes transition to the same state (i.e. ε_2, ε_4, ε_7, ε_{11}, ε_{13}). The former is triggered based on successful completion of a task within the stipulated time slot ($\beta = 60s$) whereas the latter event is triggered upon failure to complete the task defined for the given state within the stipulated time.

It is triggered to assist the patient to complete the task for a state. Note that β for the shoulder adduction partial range is given a stipulated time slot of 30s. The variables q represent the current angular position of the joints (i.e. elbow or shoulder joint). q_i denote the position of the joint just before entry to the state, thus $q - q_{Q_i} > \lambda$ denote the difference in the joint angle position upon exiting the state Q_i,. λ is the maximum allowable range of motion for the given reaching task. t represent the total time taken for a task, where F is the flag that signals the execution of a task. Overall, three logics enable inter-state transition ($q - q_{Q_i} > \lambda$, t $> \beta$, and $F = \epsilon_1$) as shown in Table 5. In each state the patient's functional activity *FA* is computed which is made available upon transiting the state (transition action).

Fig 5. The finite-state hybrid automaton architecture. Rounded rectangles represent finite states while arrow lines represent transitions. The initial state is marked Q_0 with an incoming arrow to the state. ε_i represent the state transition function or jump as given in Table 5. Half-range shoulder adduction is performed by transiting states: Q_0, Q_1 and Q_2 with transition logics $\varepsilon_0, \varepsilon_1, \varepsilon_2, \varepsilon_3, \varepsilon_4$, while full-range shoulder adduction is performed by transiting the states:

Q_2, Q_0 and Q_3 with the state transition logics: ε_5, ε_6, ε_7, ε_8. Full-range shoulder abduction is represented by states: Q_0 and Q_2 with state transition logic, ε_4; full elbow extension is represented by states: Q_0 and Q_4 with the state transition: $\varepsilon_0, \varepsilon_{10}, \varepsilon_{11}$; and full range elbow flexion is represented by states: Q_5 and Q_6 with the state transition: $\varepsilon_{12}, \varepsilon_{13}, \varepsilon_{14}$.

IV. EXPERIMENT

A. SUBJECTS

This study was approved by the IIUM research Ethics committee (IREC). Fifteen hemiplegic patients were recruited from the IIUM Physiotherapy & Rehabilitation Clinic, Kuantan, Malaysia and Heritage Physiotherapy Rehab, in May 2019, within the timeframe of study. The case file of each patient was documented before the experimental session. Details of the patients' pathologies are given in Table 7. Generally, inclusion criteria required patients to be right hemiplegic manifesting limited range of movement on the shoulder and elbow joint. All participants willingly gave their consent to participate in the experiment and were shown how to use the robotic device.

B. EXPERIMENT PROTOCOL

The clinical experiment is divided into two tasks: (Task 1) pick-and-place reaching task and (Task 2) table-to-mouth reaching task. Each task starts with an evaluation trial where the exoskeleton robot is operated in passive mode. The evaluation allows to preliminarily determine the patient functional

TABLE 7. Post stroke patients' details.

Patient ID	Age	Weight (Kg)	Patient Condition	Duration of Disability
1	65	90	Right Hemiplegia. Weak UL and LL	One year
2	75	73	Right Hemiplegia. Weak UL	One year
3	32	77	Right Hemiplegia. Weak UL and LL	One year and half
4	42	91	Right Hemiplegia. Weak UL	Six-months
5	57	70	Right Hemiplegia. Weak UL and LL	Eleven months
6	81	63	Right Hemiplegia. Weak UL	Ninth months
7	66	55	Right Hemiplegia. Weak UL	One year and ninth months
8	80	69	Right Hemiplegia. Weak UL and LL	Two years and seven months
9	67	65	Right Hemiplegia. Weak UL and LL)	One year and half
10	27	84	Right Hemiplegia. Weak UL	Two year
11	42	88	Right Hemiplegia. Weak UL	One year and two months
12	65	95	Right Hemiplegia. Weak UL and LL	One year
13	55	120	Stroke (hemiplegic)	Eight months
14	51	67	Right Hemiplegia. Weak both side ULR ULL)	Two years and ten months
15	66	70	Right Hemiplegia. Weak UL	One year and three months

UL – Upper limb, LL- Lower limb, ULR – Upper limb right, ULL – Upper limb left

ability and to set a reference assistive torque (Eqn. 9) for the subsequent trials.

1) TASK 1

The pick-and-place reaching task involves shoulder abduction/adduction movement performed in accordance with clinical procedure [38]. Under this task, each patient is instructed to pick a bottle (weighing 340g) from one table position to another position while wearing/supported by the exoskeleton robot. The device provides some resistance to patient's movement in the passive evaluation mode and assistance-as-needed in the active mode.

2) TASK 2

The Table-to-mouth reaching task involves elbow flexion and extension movement where each patient is required to hold/grasp a bottle of water weighing 340g from table position and move the bottle to the mouth while wearing the exoskeleton robot.

V. RESULTS AND DISCUSSIONS

A. ETIMATION OF SUBJECT FUNCTIONAL ABILITY (FA)

Experiment has been conducted to validate the FA estimation algorithm (Eqn. 3) by comparing the estimated FA with standard clinical measure ARAT (Table 4) in reaching task. The robotic device is powered down to ensure only patients' effort is provided to perform the task without assistance from the device (while estimating the patients' functional movement ability). Fig 6 and Fig. 7 show the plot of the quality of movement, QoM ($\emptyset_p$) and time score, TS ($\emptyset_t$) for some patients performing pick-and-place (Task 1) and table-to-mouth (Task 2) reaching tasks. It is clear that the FA algorithms put these patients at different functional capability a level which is closely related to their scores in the ARAT measurement scale (Table 6). Average functional ability estimates for patients labeled as (Patient 1) and other patients donated as patient (patient 2) are with a mean score of $FA_{Patients1} = 2.96$ and $FA_{Patients2} = 0.78$. Also, for patients (patient 3 and patient 4) the average functional ability is $FA_{Patients3} = 3.20$ and $FA_{Patient4} = 0.34$ which approximates to their clinical rating (by therapist) of 3 and 1 using the ARAT scale.

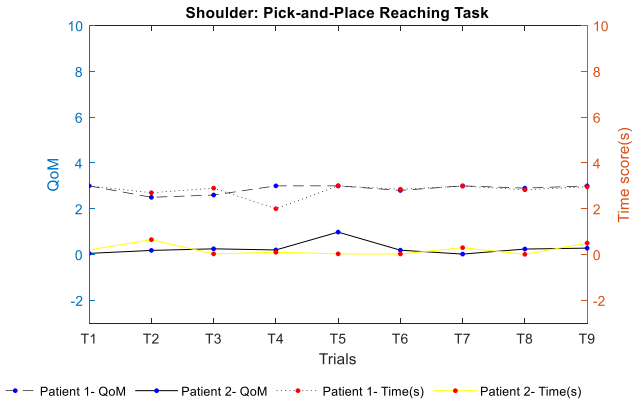

FIGURE 6. The plot of the quality of movement, QoM ($\emptyset_p$) and time score, TS ($\emptyset_t$) for two patients performing Pick-and-Place reaching task.

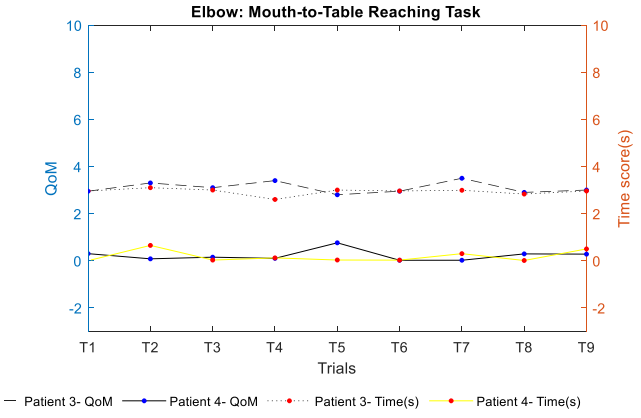

FIGURE 7. The plot of the quality of movement, QoM ($\emptyset_p$) and time score, TS ($\emptyset_t$) for two patients performing Table-to-Mouth reaching task.

The FA algorithm uses patients' quality of movement, and time score in a z-spline approximation function which is much related to the clinical procedure. The current scheme thus avoids the limitations of some of the previous studies like the method proposed by [8] in which subjects' movement capabilities are dependent on noisy force estimation

that could erroneously judge patient's functional ability. The current scheme thus offers the advantage to allow appropriate progression of therapeutic assistance especially for therapies like AAN where assistance is tailored to subjects' capabilities in reaching task. The results proved that the formulated FA using spline function is successful in estimating the patient's level of capability accurately as in the real clinical procedure done by therapists.

B. VALIDATION OF AAN CONTROLLER

This section gives results of validation experiments for the overall AAN controller. The controller consists of three main algorithms: FA estimation algorithm, FA-to-Torque mapping algorithms, and the LQGi torque controller. Since the validation of FA estimation has been demonstrated in Section V(A), the results in this section highlights the verification of the other algorithms and the overall AAN controller performance. We consider the AAN controller performance (result) for Task 1 and Task 2 in three different case studies: (1) torque assistance performance across trials for all patients, (2) torque assistance for severe disability, and (3) torque assistance for mild disability. Each experiment and the results demonstrates how patient's FA is estimated and how it is applied to adjust robotic assistance.

1) TORQUE ASSISTANCE ACROSS TRIALS

Fig. 8. and 9. show the plot of assistive torques across trials for all the participants in both tasks. $T_1, T_2 \ldots T_n$ represent the number of trials performed for each task. A total of 9 trials are performed by each participant where all trials are preceding by an evaluation trial, T_1, performed to set the reference torque for the second trial. After the second trial, the FA is estimated and used to set the robot assistance for the third trial. The subsequent trials proceed in the same fashion. For all the reaching tasks, variability in the torque assistance is clearly seen across all trials in accordance with the estimated

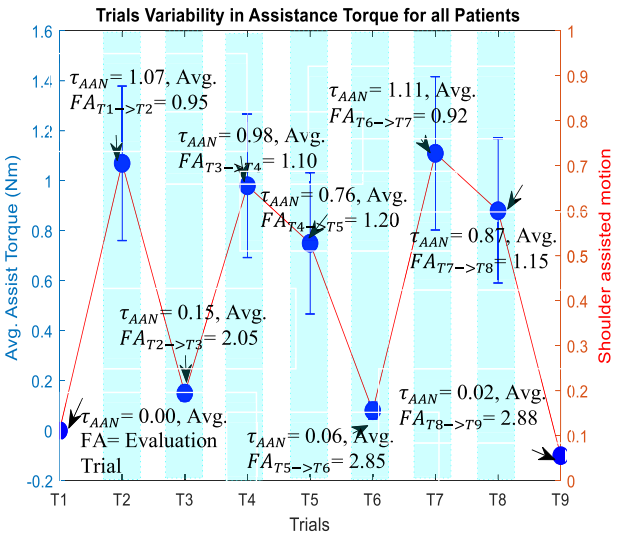

FIGURE 8. The plot of assistive torques across all trials (Shoulder activities) [mean FA = 1.37].

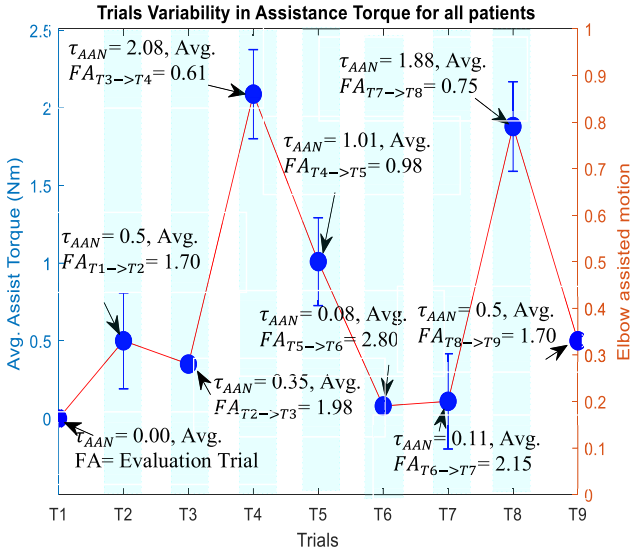

FIGURE 9. The plot of assistive torques across all trials [mean FA = 1.40].

patients' FA (Eqn. 3). Error bars show standard error of the mean of assistance torque for all the participants. Starting at T2 (Fig. 8), the torque assistance (τ_{AAN} =1.07Nm) provided to the patients to complete the task is set by the estimated FA ($FA_{T1->T2}$ =0.95) in the previous evaluation task, T1. Consequently, the estimated FA of the patient after the trial (T2) is completed, i.e. $FA_{T2->T3}$ =2.05, is significantly improved due to the robotic assistance (influenced by the assistance provided by the robotic device). This FA is applied to set the assistance in the next trial T3 (i.e. τ_{AAN} = 0.15Nm). This procedure is repeated throughout the subsequent trials. An important point to mention here is that rather than subtracting the previous/evaluation FA estimated in a trial from the current FA to adjust the torque, we make no modification in this respect in order to prevent slacking behavior.

The FA estimation algorithm (Eqn. 3) guarantees an inverse (torque) relationship to the patient's FA, thus if the estimate of patient's FA, when robotic assistance is provided, is high (potentially because of the assistance), the torque assistance provided for the next task would be low to encourage/promote patients' involvement. This trend is equally noticeable for all the patients in the table-to-mouth reaching task (Fig. 9). Notice that, the robotic assistance provided to the patients are also supported by therapist's instructions to motivate or encourage or promote patient participation and compliance with the therapy objective. In AAN encourage means to promote patient's participation when the assistance is decreased [14]–[16], [18], [19], [39]. Without instructions from the therapists, patients also tend to reduce their effort to participate.

2) TORQUE ASSISTANCE FOR SEVERE DISABILITY: CASE 1 PICK AND PLACE

The performance of the AAN torque assistance strategy for two cases of severely disabled patients performing pick

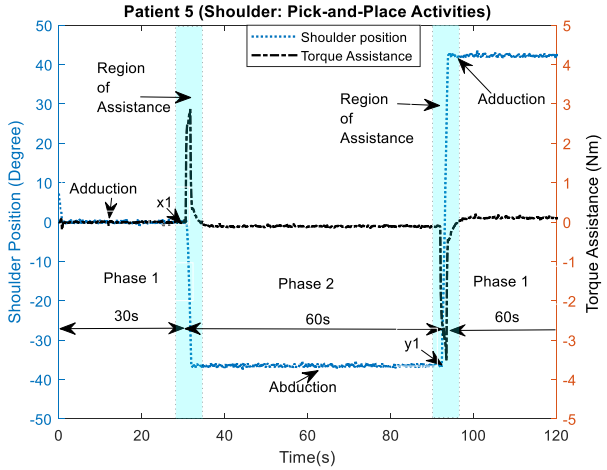

FIGURE 10. Plot of shoulder position and torque assistance vs time for pick and place activities. The severe patients in this case have limited range of motion.

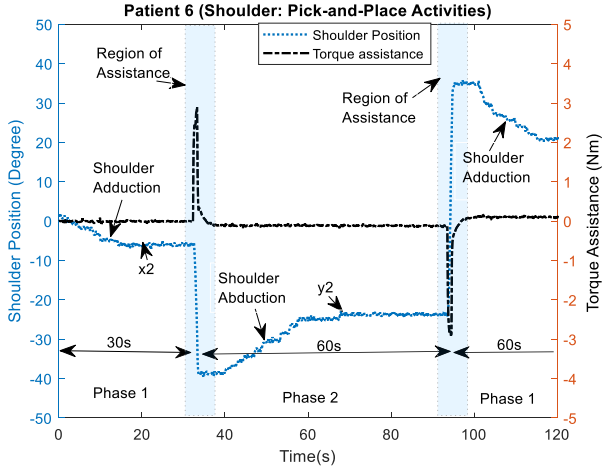

FIGURE 11. Plot of shoulder position and torque assistance vs time for pick and place activities. The severe patients in this case have some range of motion.

and place (PAP) reaching task is shown in Fig.10, and 11, Blue bold line represents shoulder position and broken line denote torque assistance. The reaching task is divided into two phases: (1) PAP involving shoulder abduction, and (2) PAP involving shoulder adduction movements (Fig.10.). The severe participants in this case have limited range of motion and thus unable to fully perform the reaching tasks in both phases. In phase (1), one of the patients (Patient 5) show only slight movement of the limb despite effort to move the arm; he is thus assisted $\tau_{AAN} = 3.0$Nm) by the FA-AAN strategy after 30s of unsuccessful attempt to complete the task (see region marked 'x_1' in Fig.10.). The 30s is stipulated here since a half ROM is covered from initial position to full shoulder adduction. The second patient (Patient 6) could only abduct the limb to certain degree (see point marked 'x_2' in Fig.11) with obvious difficulty in completing the full ROM. Consequently, the controller provide assistance ($\tau_{\text{AAN}} = 2.8$Nm) to the patient after a total of 30s (half adduction ROM) time lapse. Performance of the both patients in phase (2) is similar to their respective performance in phase 1. Assistance is provided to the patients by the FA-AAN after 60s of unsuccessful attempt to complete the task. Shoulder adduction assistance torque is denoted positive under the assistance scheme, while abduction is denoted negative. Table 8 show summary of the torque assistance profile. As expected, the assistance torque provided to the first patient (who show no functional capability) is higher than the one provided to the second patient (who exhibited some functional capability), which show that the FA-AAN controller responded appropriately to the patient's function ability.

TABLE 8. Summary of the torque assistance profile.

Task	Case study	Description	FA score	Avg. Torque Assist (Nm)	Avg. Torque assistance (%) *	Avg. time
Pick and place	Case 1	Severe 1	0	+3.00 Nm	85.71%	> 30s
			0	-3.40 Nm	97.14%	> 60s
		Severe 2	1	+2.8 Nm	80.00%	30s
			1	-3.01 Nm	86.00%	60s
	Case 2	Mild 1	2.1	±0.58Nm	16.57%	16s
		Mild 2	1.8	±0.87 Nm	24.85 %	21s
Table to Mouth	Case 1	Severe 1	0	-2.89 Nm	82.57%	> 60s
		Severe 2	1	-2.63 Nm	75.14%	60s
	Case 2	Mild 1	2.2	+0.40Nm	11.42%	14s
		Mild 2	2.5	± 0.19 Nm	5.43%	11s

* Avg. Torque (%) = $(Avg.\ Torque\ Assist)\ /\ (Max.Torque)$
Max. Torque is =3.50Nm.

3) TABLE-TO-MOUTH REACHING TASK

Fig.12 and 13. show the assistance modality of the FA-AAN in table-to-mouth reaching task for two neurologically impaired participants with limited capability for elbow flexion movement. Similarly, torque assistance is provided to the patients after 60s of unsuccessful attempt to complete the table-to-mouth activity. Whereas one of the patients (Patient 7) could not physically move his arm, the second patient (Patient 8) is able to attain a maximum ROM marked x_1, beyond which was physically difficult to move. The green shade show region where torque assistance is provided to assist the patient to complete the task. A maximum torque assistance of (2.89Nm) is provided to the first patient (Patient 7) to complete the task which correlates with the calculated FA score (FA = 0) of patient's performance. The second patient (Patient 8) show some degree of functional capability in the task, although he/she is unable to complete the task at a certain range of elbow flexion/extension

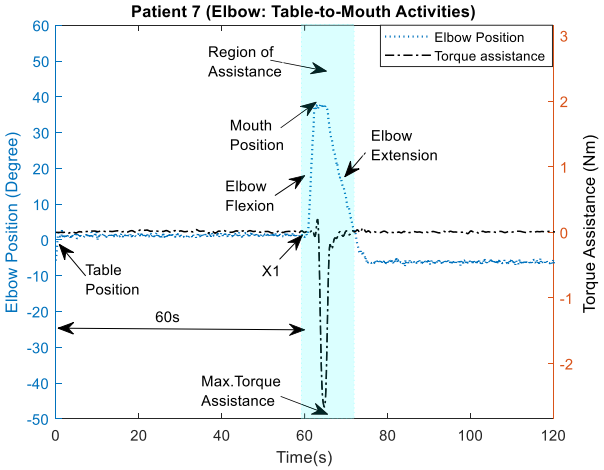

FIGURE 12. Plot of elbow position and torque assistance vs time for Table-to-Mouth activities. The severe patients in this case have limited range of motion.

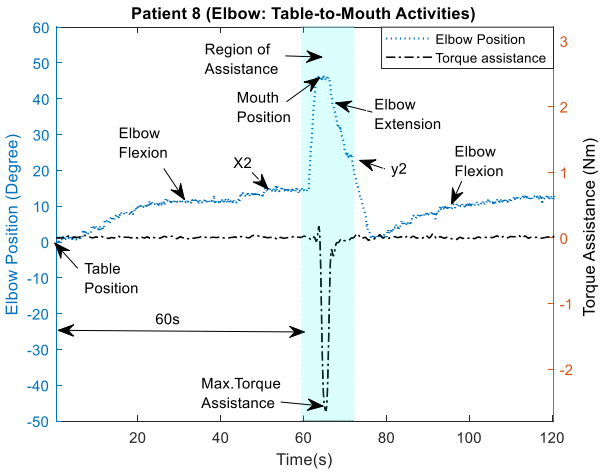

FIGURE 13. Plot of elbow position and torque assistance vs time for Table-to-Mouth activities. The severe patients in this case have some range of motion.

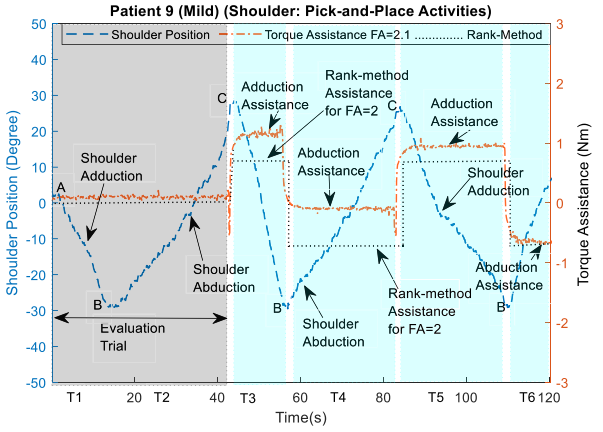

FIGURE 14. Assistive torque vs. shoulder position for mild disabled patients.

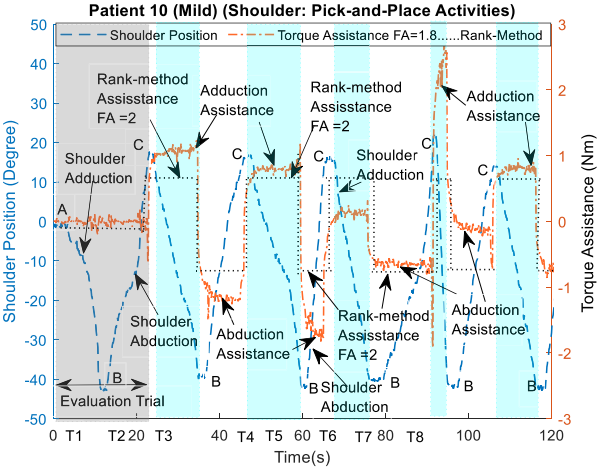

FIGURE 15. Assistive torque vs. shoulder position for mild disabled patients.

denoted 'x_2' and 'y_2' respectively. Consequently, the controller provided assistance to the patient to complete the task after 60s count out with approximately (τ_{AAN} =2.63Nm) torque assistance which correlates with the patient FA score (FA =1).

Notice that 60s has been used as the maximum limit allowable for a trial and evaluation based on popular clinical scale ARAT for severely disabled patients [40], [41]. According to ARAT scale implemented in clinical practice, the time before assistance is set to be 60s for severely disabled patients, Under the AAN scheme, the idea is that patients are encouraged or promoted to make effort to prevent slacking behavior (i.e. to prevent relying completely on robotic assistance as in the case of passive training) within an allowable time threshold.

4) TORQUE ASSISTANCE FOR MILD DISABILITY: CASE 2 PICK AND PLACE REACHING TASK

Fig.14. and 15. show the plots of assistive torque vs. shoulder position for two mild disabled patients with FA scores of 2.1 and 1.8. The exercise trial proceeds first with an evaluation phase then followed with the assistance phase. Patients' movement ability is monitored and computed in the evaluation phase to stipulate a reference working torque for the subsequent phase. This procedure is also adopted for the case of severely disabled discussed above. The patient is able to complete the reaching task but overall, torque assistance provided to the two patients (Patient 9 and Patient 10) are lower compared to the case of severely disabled patients in Case 1. Average assistive torque for Mild 1 patient (with FA=2.1) is 0.58Nm which is 16.57% of maximum assistive torque in the current scheme (Table 8). Notice that the maximum assist torque in our current scheme is 3.5Nm which is the torque provided to assist the severely disabled patients (FA=0). On the other hand, the average assist torque of Mild 2 patient (with FA=1.8) is 0.87 Nm which is 24.85% of the maximum assist torque. Thus, we see that average assist torque provided to Mild 2 (which has slightly lower functional ability) is about 8.28 % higher than that provided to Mild 1, under

the current scheme, given the difference in their FAs. Higher torque enables faster task completion.

Fig 14 and Fig 15 also compares the results of Mild 1 and Mild 2 with ranked method. Black dotted lines show the results of the ranked method. Under ranked method, Mild 1 and Mild 2 will be given the same rank as FA=2, and provided the same torque of 0.70Nm. In comparison to ranked method the assist performance for FA=1.8 improves by 22% and for FA = 2.1, the assist performance improves by 17%.

Overall, the ranked method is useful and can be an approximation for our proposed method, it is however not capable to adapt to slight difference in patients' disability level which is an important principle in Assist-as-needed rehabilitation scheme that has been proposed in our current method.

5) TABLE TO MOUTH REACHING TASK

Fig.16. and 17. show the plots of assistive torque vs elbow position for two patients (FA=2.2 and FA = 2.5) with mild disability for elbow flexion/extension motion. Torque assistance provided to the patients are lower compared to the assistance provided for case of severely disable patients in Case 1, see Table 8. Both patients could complete the reaching task but at different times (Table 8). Average assistive torque provided to the first patient (Patient 11, with FA =2.2) for elbow flexion and extension motion is approximately −0.33Nm and +0.40Nm respectively. For the second patient (Patient 12, FA=2.5), torque assistance for elbow flexion and extension is −0.19Nm and +0.2Nm respectively. Overall, patients' scores in any phase is carried over to the subsequent phase to stipulate a baseline assistive torque. The evaluation phase is always unassisted.

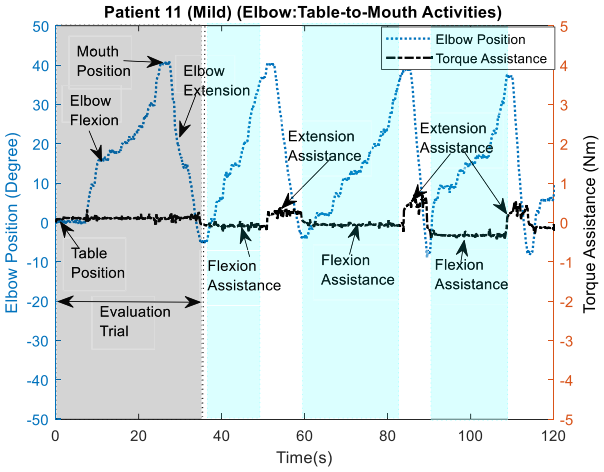

FIGURE 16. Assistive torque vs elbow position for mild patients.

In the case of mild patients, they can move their shoulder/elbow within less than 60s, where the robot assists the patients immediately according to ARAT assessment test implemented in an actual clinical practice. This can be seen in Figs 14-17. It would be observed in Fig 15 that after time t=20s, i.e. after the evaluation period, robotic assistance is provided immediately for each trial for mild patients

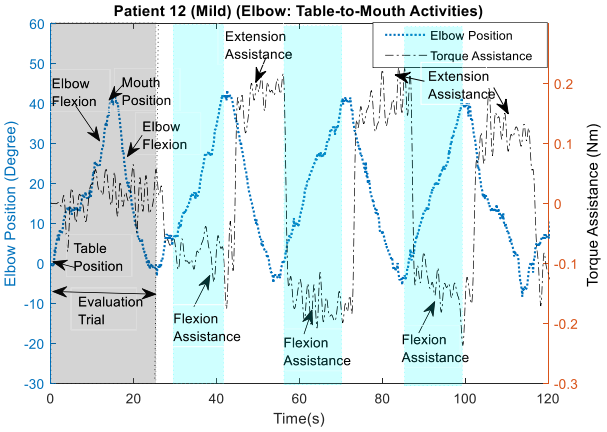

FIGURE 17. Assistive torque vs elbow position for mild patients.

TABLE 9. Nomenclature lists (symbols and definitions).

Symbol	Description
AAN	Assist-as-needed
FA	functional ability
FASF	Functional Activity Spline Function
LQGi	Linear Quadratic Gaussian Integral
ADL	activities of daily living
mAAN	minimal assist-as-needed
ARAT	Action Research Arm Test
WMFT	Wolf Motor Function Test
AA	abduction/adduction
FE	flexion/extension
PS	pronation/supination
QoM	Quality of movement
zmf	z-spline function
IREC	IIUM research Ethics committee
IIUM	International Islamic University Malaysia
UL	Upper limb
LL	Lower limb
TS	Time score
T_i,	Trial
PAP	Pick and place
TTM	Table to mouth
ROM	Range of motion
FA-AAN	functional ability -to-torque mapping algorithm

(task involve shoulder abd/add) and this goes on continuously. Evaluation time for each mild participant only last until the patient can complete the task which is only for few seconds.

VI. CONCLUSION

In this article an Assist-as-Needed (AAN) control strategy based on a new functional activity spline function (FASF) is proposed for patients with various degrees of shoulder and elbow disability. The FASF algorithm has been validated and found consistent with clinical procedure, such as the ARAT measurement scale adopted in this study. Overall, the controller is found to automate robotic assistance based on patients' FASF estimation.

Performance of the controller has also been validated in three different scenarios on patients with severe and mild movement disability on the shoulder and elbow regions.

The FA-AAN strategy accurately and consistently provided robotic assistance, in varying amount to each case of disability. The results show the feasibility of the proposed FA-AAN for actual rehabilitation therapy.

Future work will include a virtual reality gaming console to provide external instruction for motivating the patients to participate in the therapy, similar to the role of a human therapist.

ACKNOWLEDGMENT

The authors gratefully acknowledge the Rehabilitation Unit, IIUM Medical Centre for their assistance with this research.

REFERENCES

[1] M. H. Al-Eithan, M. Amin, and A. A. Robert, "The effect of hemiplegia/hemiparesis, diabetes mellitus, and hypertension on hospital length of stay after stroke," *Neurosciences (Riyadh)*, vol. 16, no. 3, pp. 253–256, 2011.

[2] S. M. Hatem, G. Saussez, M. D. Faille, V. Prist, X. Zhang, D. Dispa, and Y. Bleyenheuft, "Rehabilitation of motor function after stroke: A multiple systematic review focused on techniques to stimulate upper extremity recovery," *Frontiers Hum. Neurosci.*, vol. 10, p. 442, Sep. 2016.

[3] L. A. Pilutti, D. A. Lelli, J. E. Paulseth, M. Crome, S. Jiang, M. P. Rathbone, and A. L. Hicks, "Effects of 12 weeks of supported treadmill training on functional ability and quality of life in progressive multiple sclerosis: A pilot study," *Arch. Phys. Med. Rehabil.*, vol. 92, no. 1, pp. 31–36, Jan. 2011.

[4] H. Rodgers *et al.*, "Robot assisted training for the upper limb after stroke (RATULS): A multicentre randomised controlled trial," *Lancet*, vol. 394, pp. 51–62, Jul. 2019.

[5] S. Y. A. Mounis, N. Z. Azlan, and S. Fatai, "Progress based assist-as-needed control strategy for upper-limb rehabilitation," in *Proc. IEEE Conf. Syst., Process Control (ICSPC)*, Dec. 2017, pp. 65–70.

[6] K. Nas, L. Yazmalar, V. Sah, A. Aydin, and K. Önes, "Rehabilitation of spinal cord injuries," *World J. Orthopedics*, vol. 6, no. 1, p. 8, 2015.

[7] P. Flachenecker, "Clinical implications of neuroplasticity–the role of rehabilitation in multiple sclerosis," *Frontiers Neurol.*, vol. 6, p. 36, Mar. 2015.

[8] A. U. Pehlivan, D. P. Losey, and M. K. OMalley, "Minimal Assist-as-Needed controller for upper limb robotic rehabilitation," *IEEE Trans. Robot.*, vol. 32, no. 1, pp. 113–124, Feb. 2016.

[9] A. Houwink, R. H. Nijland, A. C. Geurts, and G. Kwakkel, "Functional recovery of the paretic upper limb after stroke: Who regains hand capacity?" *Arch. Phys. Med. Rehabil.*, vol. 94, no. 5, pp. 839–844, May 2013.

[10] L. M. Muratori, E. M. Lamberg, L. Quinn, and S. V. Duff, "Applying principles of motor learning and control to upper extremity rehabilitation," *J. Hand Therapy*, vol. 26, no. 2, pp. 94–103, Apr. 2013.

[11] S. A. Billinger, R. Arena, J. Bernhardt, J. J. Eng, B. A. Franklin, C. M. Johnson, M. MacKay-Lyons, R. F. Macko, G. E. Mead, E. J. Roth, M. Shaughnessy, and A. Tang, "Physical activity and exercise recommendations for stroke survivors: A statement for healthcare professionals from the American heart association/American stroke association," *Stroke*, vol. 45, no. 8, pp. 2532–2553, Aug. 2014.

[12] C. Y. Looi, M. Duta, A.-K. Brem, S. Huber, H.-C. Nuerk, and R. Cohen Kadosh, "Combining brain stimulation and video game to promote long-term transfer of learning and cognitive enhancement," *Sci. Rep.*, vol. 6, no. 1, p. 22003, Apr. 2016.

[13] K. Hötting and B. Röder, "Beneficial effects of physical exercise on neuroplasticity and cognition," *Neurosci. Biobehavioral Rev.*, vol. 37, no. 9, pp. 2243–2257, Nov. 2013.

[14] A. A. Blank, J. A. French, A. U. Pehlivan, and M. K. O'Malley, "Current trends in robot-assisted upper-limb stroke rehabilitation: Promoting patient engagement in therapy," *Current Phys. Med. Rehabil. Rep.*, vol. 2, no. 3, pp. 184–195, Sep. 2014.

[15] S. Hussain, P. K. Jamwal, M. H. Ghayesh, and S. Q. Xie, "Assist-as-Needed control of an intrinsically compliant robotic gait training orthosis," *IEEE Trans. Ind. Electron.*, vol. 64, no. 2, pp. 1675–1685, Feb. 2017.

[16] L. Luo, L. Peng, C. Wang, and Z.-G. Hou, "A greedy assist-as-needed controller for upper limb rehabilitation," *IEEE Trans. Neural Netw. Learn. Syst.*, vol. 30, no. 11, pp. 3433–3443, Nov. 2019.

[17] N. Rehmat, J. Zuo, W. Meng, Q. Liu, S. Q. Xie, and H. Liang, "Upper limb rehabilitation using robotic exoskeleton systems: A systematic review," *Int. J. Intell. Robot. Appl.*, vol. 2, no. 3, pp. 283–295, 2018.

[18] J. M. Frullo, "Effects of assist-as-needed upper extremity robotic therapy after incomplete spinal cord injury: A parallel-group controlled trial," *Frontiers Neurorobot.*, vol. 11, p. 26, Jun. 2017, doi: 10.3389/fnbot.2017.00026.

[19] L. Peng, C. Wang, L. Luo, S. Chen, Z.-G. Hou, and W. Wang, "A CPG-inspired assist-as-needed controller for an upper-limb rehabilitation robot," in *Proc. IEEE Symp. Ser. Comput. Intell. (SSCI)*, Nov. 2018, pp. 2200–2206.

[20] L. De Vito, O. Postolache, and S. Rapuano, "Measurements and sensors for motion tracking in motor rehabilitation," *IEEE Instrum. Meas. Mag.*, vol. 17, no. 3, pp. 30–38, Jun. 2014.

[21] H. I. Krebs, J. J. Palazzolo, L. Dipietro, M. Ferraro, J. Krol, K. Rannekleiv, B. T. Volpe, and N. Hogan, "Rehabilitation robotics: Performance-based progressive robot-assisted therapy," *Auton. Robots*, vol. 15, no. 1, pp. 7–20, 2003.

[22] N. Hogan, H. I. Krebs, B. Rohrer, J. J. Palazzolo, L. Dipietro, S. E. Fasoli, J. Stein, R. Hughs, W. R. Frontera, D. Lynch, and B. T. Volpe, "Motions or muscles? Some behavioral factors underlying robotic assistance of motor recovery," *J. Rehabil. Res. Develop.*, vol. 43, no. 5, p. 605, 2006.

[23] E. Papaleo, L. Zollo, L. Spedaliere, and E. Guglielmelli, "Patient-tailored adaptive robotic system for upper-limb rehabilitation," in *Proc. IEEE Int. Conf. Robot. Automat.*, May 2013, pp. 3860–3865.

[24] E. Vergaro, M. Casadio, V. Squeri, P. Giannoni, P. Morasso, and V. Sanguineti, "Self-adaptive robot training of stroke survivors for continuous tracking movements," *J. NeuroEng. Rehabil.*, vol. 7, no. 1, p. 13, Dec. 2010.

[25] J. C. Pérez-Ibarra, A. A. G. Siqueira, and H. I. Krebs, "Assist-as-needed ankle rehabilitation based on adaptive impedance control," in *Proc. IEEE Int. Conf. Rehabil. Robot. (ICORR)*, Aug. 2015, pp. 723–728.

[26] E. T. Wolbrecht, V. Chan, D. J. Reinkensmeyer, and J. E. Bobrow, "Optimizing compliant, model-based robotic assistance to promote neurorehabilitation," *IEEE Trans. Neural Syst. Rehabil. Eng.*, vol. 16, no. 3, pp. 286–297, Jun. 2008.

[27] C. Bower, H. Taheri, and E. Wolbrecht. "Adaptive control with state-dependent modeling of patient impairment for robotic movement therapy," in *Proc. IEEE 13th Int. Conf. Rehabil. Robot. (ICORR)*, Jun. 2013, pp. 1–6

[28] R. Huang, H. Cheng, Q. Chen, H.-T. Tran, X. Lin, "Interactive learning for sensitivity factors of a human-powered augmentation lower exoskeleton," in *Proc. IEEE/RSJ Int. Conf. Intell. Robots Syst. (IROS)*, Sep./Oct. 2015, pp. 6409–6415,

[29] C. Obayashi, T. Tamei, and T. Shibata, "Assist-as-needed robotic trainer based on reinforcement learning and its application to dart-throwing," *Neural Netw.*, vol. 53, pp. 52–60, May 2014.

[30] Q. Liu, A. Liu, W. Meng, Q. Ai, and S. Q. Xie, "Hierarchical compliance control of a soft ankle rehabilitation robot actuated by pneumatic muscles," *Frontiers Neurorobotics*, vol. 11, p. 64, Dec. 2017.

[31] F. Sado, H. J. Yap, R. A. R. Ghazilla, and N. Ahmad, "Exoskeleton robot control for synchronous walking assistance in repetitive manual handling works based on dual unscented Kalman filter," *PLoS ONE*, vol. 13, no. 7, Jul. 2018, Art. no. e0200193.

[32] O. Nelles, *Nonlinear System Identification: From Classical Approaches to Neural Networks and Fuzzy Models*. Springer, 2013.

[33] J. Whitall, D. N. Savin, M. Harris-Love, and S. M. Waller, "Psychometric properties of a modified wolf motor function test for people with mild and moderate upper-extremity hemiparesis," *Arch. Phys. Med. Rehabil.*, vol. 87, no. 5, pp. 656–660, May 2006.

[34] J.-L. Zhao, P.-M. Chen, W.-F. Li, R.-H. Bian, M.-H. Ding, H. Li, Q. Lin, Z.-Q. Xu, Y.-R. Mao, and D.-F. Huang, "Translation and initial validation of the chinese version of the action research arm test in people with stroke," *Biomed. Res. Int.*, vol. 2019, Jan. 2019, Art. no. 5416560.

[35] T. M. Hodics, K. Nakatsuka, B. Upreti, A. Alex, P. S. Smith, and J. C. Pezzullo, "Wolf motor function test for characterizing moderate to severe hemiparesis in stroke patients," *Arch. Phys. Med. Rehabil.*, vol. 93, no. 11, pp. 1963–1967, Nov. 2012.

[36] J. H. van der Lee, L. D. Roorda, H. Beckerman, G. J. Lankhorst, and L. M. Bouter, "Improving the action research arm test: A unidimensional hierarchical scale," *Clin. Rehabil.*, vol. 16, no. 6, pp. 646–653, 2002.

[37] S. Y. A. Mounis, N. Z. Azlan, and F. Sado, "Assist-as-needed control strategy for upper-limb rehabilitation based on subject's functional ability," *Meas. Control*, vol. 52, nos. 9–10, pp. 1354–1361, 2019.

[38] T. Platz, C. Pinkowski, F. van Wijck, I.-H. Kim, P. di Bella, and G. Johnson, "Reliability and validity of arm function assessment with standardized guidelines for the Fugl-Meyer test, action research arm test and box and block test: A multicentre study," *Clin. Rehabil.*, vol. 19, no. 4, pp. 404–411, Jun. 2005.
[39] A. S. Niyetkaliyev, S. Hussain, M. H. Ghayesh, and G. Alici, "Review on design and control aspects of robotic shoulder rehabilitation orthoses," *IEEE Trans. Human-Machine Syst.*, vol. 47, no. 6, pp. 1134–1145, Dec. 2017.
[40] R. C. Lyle, "A performance test for assessment of upper limb function in physical rehabilitation treatment and research," *Int. J. Rehabil. Res.*, vol. 4, no. 4, pp. 483–492, 1981.
[41] N. Yozbatiran, L. Der-Yeghiaian, and S. C. Cramer, "A standardized approach to performing the action research arm test," *Neurorehabilitation Neural Repair*, vol. 22, no. 1, pp. 78–90, 2008.

SHAWGI Y. A. MOUNIS received the B.S. and M.S. degrees in mechatronics engineering from International Islamic University Malaysia, Kuala Lumpur, Malaysia, in 2011 and 2015, respectively, where he is currently pursuing the Ph.D. degree with the Mechatronic Engineering Department. He is also a member with the Biomechatronic Laboratory. His research interests include robot-aided neurorehabilitation, exoskeletal robotic device design, nonlinear control, robotics, and mechatronics.

NORSINNIRA ZAINUL AZLAN (Member, IEEE) received the bachelor's degree (Hons.) in mechatronics engineering from International Islamic University Malaysia (IIUM), in 2003, and the master's and Ph.D. degrees in mechanical and control engineering from the Tokyo Institute of Technology, Japan. She is currently a Lecturer with IIUM. Her research interests include nonlinear control, upper limb rehabilitation robots, artificial prosthetics hands, and robot manipulators and automations.

FATAI SADO (Member, IEEE) received the M.Sc. degree in mechatronics engineering and the Ph.D. degree from the University of Malaya, Malaysia, in 2015 and 2019, respectively. He is currently a Researcher with the Research Management and Innovation Complex, University of Malaya. His research interests include automation and control of exoskeleton robots for rehabilitation, augmentation, and assistive purposes.